

Two-photon excitation laser scanning microscopy of porcine nasal septal cartilage following Nd:YAG laser mediated stress relaxation

Charlton C. Kim^{*a,b}, Vincent Wallace^b, Alexandre Rasouli^b, Mariah Coleno^b,
Xavier Dao^b, Bruce Tromberg^b, Brian J.F. Wong^b

^aYale University School of Medicine, New Haven, CT 06510
^bBeckman Laser Institute and Medical Clinic, Irvine, CA 92612

ABSTRACT

Laser irradiation of hyaline cartilage result in stable shape changes due to temperature dependent stress relaxation. In this study, we determined the structural changes in chondrocytes within porcine nasal septal cartilage tissue over a 4-day period using a two-photon laser scanning microscope (TPM) following Nd:YAG laser irradiation ($\lambda= 1.32 \mu\text{m}$) using parameters that result in mechanical stress relaxation (6.0W, 5.4 mm spot diameter). TPM excitation (780 nm) result in induction of fluorescence from endogenous agents such as NADH, NADPH, and flavoproteins in the 400-500nm spectral region. During laser irradiation diffuse reflectance (from a probe HeNe laser, $\lambda= 632.8 \text{ nm}$), surface temperature, and stress relaxation were measured dynamically. Each specimen received one, two, or three sequential laser exposures (average irradiation times of 5, 6, and 8 seconds). The cartilage reached a peak surface temperature of about 70°C during irradiation. Cartilage denatured in 50% EtOH (20 minutes) was used as a positive control. TPM was performed using a mode-locked 780nm Titanium:Sapphire (Ti:Al2O3) beam with a 63X, 1.2 N.A. water immersion objective (working distance of 200mm) to detect the fluorescence emission from the chondrocytes. Images of chondrocytes were obtained at depths up to 150 microns (lateral resolution = 35 $\mu\text{m} \times 35 \mu\text{m}$). Images were obtained immediately following laser exposure, and also after 4 days in culture. In both cases, the irradiated and non-irradiated specimens do not show any discernible difference in general shape or autofluorescence. In contrast, positive controls (immersed in 50% ethanol), show markedly increased fluorescence relative to both the native and irradiated specimens, in the cytoplasmic region.

Keywords: Cartilage, microscopy, viability, chondrocyte, two-photon

1. INTRODUCTION

In reconstructive procedures within the head and neck, autogenous cartilage grafts harvested from heterotopic sites are used to rebuild the damaged framework of facial and airway structures. Often, the graft must be carved, sutured, or morselized in order to recreate the shape of the missing structure. The drawback to these techniques is that excess normal tissue is often discarded, and significant donor site morbidity may result. As a cartilage-sparing alternative, laser irradiation can be used to reshape cartilage grafts into complex shapes, via thermal-mediated stress relaxation.

Mechanical stress relaxation occurs during laser heating; internal stress [$\sigma(t)$] (the force exerted by the cartilage resisting external deformation) initially increases, peaks, and then rapidly decreases prior to cessation of laser irradiation¹ (**Figure 1**). At the same time, diffuse reflectance $I(t)$ from a visible wavelength probe laser follows a similar temporal pattern to $\sigma(t)$, in that it too peaks and decreases. Previously, we demonstrated that non-contact optical monitoring could be used to assess real-time changes in tissue mechanical properties during laser irradiation and control the reshaping process². The peak in $I(t)$, observed during laser irradiation, indicates the onset of stress relaxation and can be used to modulate laser power or terminate irradiation.

While the biophysical changes accompanying laser reshaping have been characterized^{1,3-8}, the effect of laser irradiation on chondrocyte viability and metabolism has not been extensively studied. Conventional light microscopy has been used to examine intact irradiated cartilage specimens, however, tissue fixation and exogenous dyes are necessary, and as a result serial examination of the same specimen over time is not possible.

* correspondence: charlton.kim@yale.edu

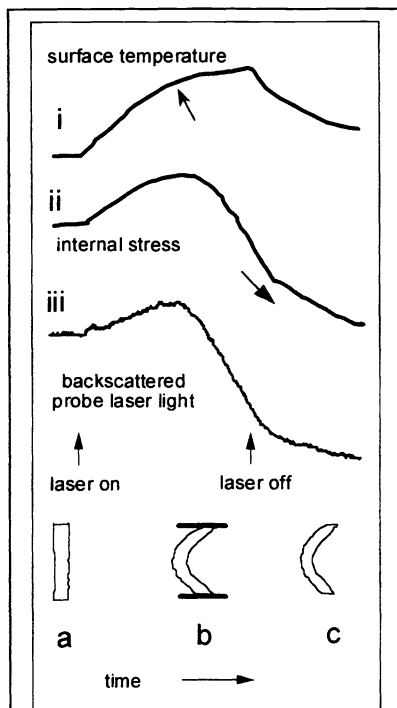


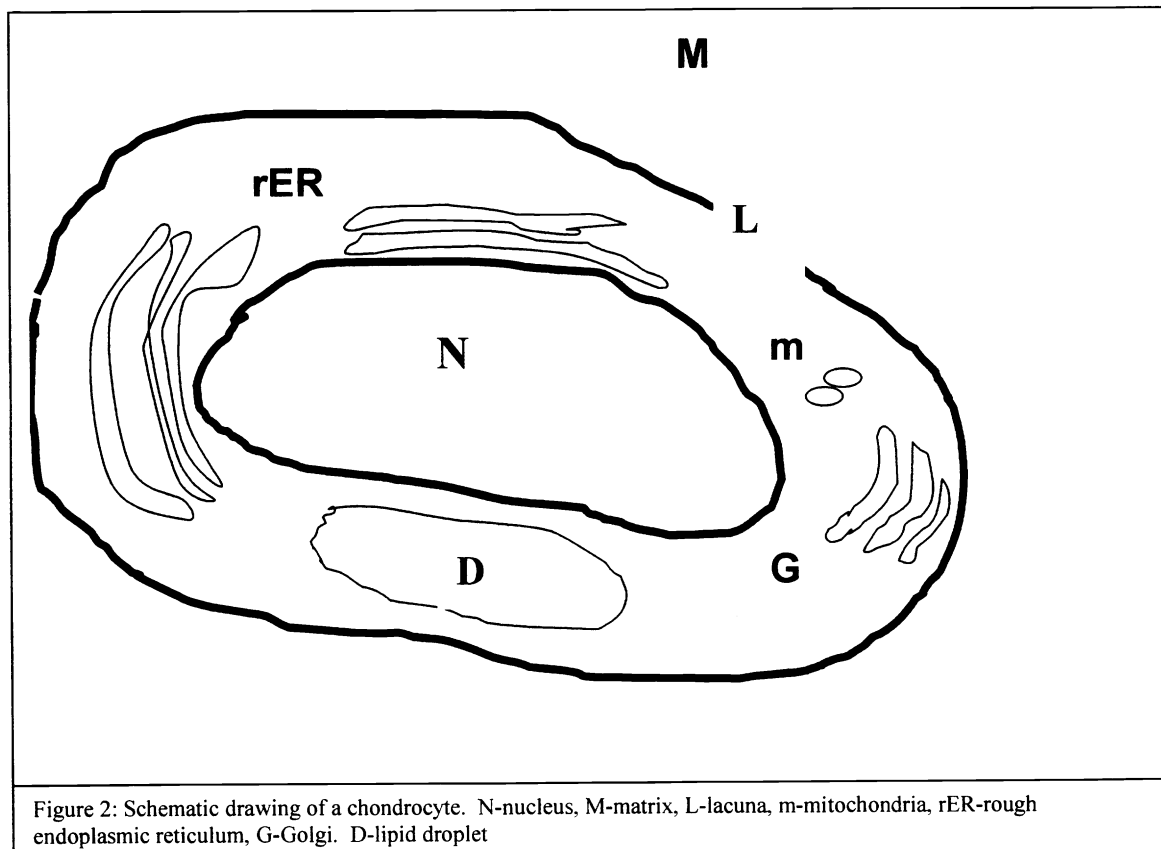
Figure 1: Laser-Mediated Cartilage Reshaping. A flat cartilage specimen (a) is held in a reshaping jig (b) during Nd:YAG laser irradiation to create a new shape (c) as surface temperature (i), internal stress (ii), and backscattered HeNe probe laser light (iii) are recorded. When surface temperature reaches about 70°C (arrow) a change in slope of the temperature curve is observed suggesting a change in tissue thermal properties. With the onset of laser irradiation, internal stress initially increases, then at 70°C, internal stress begins to rapidly decrease (large arrow) as reshaping begins (ii). Alterations in measured backscattered probe light (iii) mirror corresponding changes in internal stress.

following laser-mediated stress relaxation. Porcine nasal septum consists primarily of hyaline cartilage. Within the tissue, small chondrocyte aggregates (usually 2-4 cells) are embedded within an extensive matrix containing ground substance and collagen fibers. Chondrocytes are contained within the *lacuna*, a defect in the matrix structure (Figure 2). The matrix immediately surrounding the lacuna is often referred to as the *territorial matrix*, and contains a high concentration of acidic, sulfated proteoglycans. The intracellular structure of chondrocyte is similar to most eukaryotic cells. A well-defined nucleus is surrounded by an extensive *rough endoplasmic reticulum* and *Golgi* apparatus. In transmission electron microscopy, *nucleoli* and numerous *mitochondria* are identified. In larger chondrocytes, large lipid droplets within the cytoplasm may be a prominent feature¹⁵.

Optically thick, living tissue can be imaged using confocal laser scanning microscopy (CLSM), which overcomes many of the limitations of conventional light microscopy. However, CLSM has drawbacks including: 1) photobleaching from the high intensity laser energy, 2) phototoxicity to tissue due to high laser power, 3) relatively shallow penetration depth, 4) need for exogenous stains, and 5) often, the need for tissue fixation. In CLSM, image quality is often reduced because of the concern that excessive laser light exposure may result in photobleaching and phototoxicity of the tissue specimen. Hence, there is often a trade-off between image quality and the number of optical sections generated in a 3-dimensional image, the number of scans per image, and/or the number of scans over time⁹. While ultra-violet (UV) CLSM eliminates the need for exogenous diffusion limited fluorescent stains, the optical design is complex, expensive, and only partially compensates for inherent chromatic aberrations. Further, UV light causes significant photobleaching and photochemical toxicity.

Two Photon Laser Scanning Microscopy (TPM) is a relatively new technique that overcomes many of the limitations of both UV and conventional CLSM. In TPM, two near-infrared (NIR) photons excite fluorophores normally excited by a single photon of half the wavelength. The deeper-penetrating near-IR wavelengths excite endogenous fluorophores which would normally be stimulated only by shallow-penetrating UV photons, allowing for the generation of images at substantial depths in living tissues. Phototoxicity is reduced because excitation occurs only within the diffraction-limited focus of the beam (eliminating out-of-focus interference), and of the short pulse duration (~100fs) of the high-intensity NIR laser. The NIR laser beam is raster-scanned across a focal plane within the tissue while photomultiplier tubes (PMTs) collect emitted UV light. As a consequence, optical sections of tissue specimens at substantial depths (up to several hundred microns) are obtained, without the need for exogenous dyes and tissue fixation, and with limited phototoxicity¹⁰. Endogenous cellular fluorophores (principally NADH, NADPH, and flavoproteins) emit in the 400-500 nm region of the spectrum, and the signal intensity is proportional to the concentration of these metabolites. TPM is REDOX imaging and thus can be used to gauge cellular metabolism. TPM has been used to image such tissues as the cornea¹¹ and inner ear hair cells¹², and to image *in situ* physiological processes including glucose metabolism in pancreatic beta cells¹³ and capillary blood flow in the neocortex¹⁴. With TPM the cytoplasm/nucleus interface is imaged with high resolution. Dividing cells can be distinguished from quiescent cells, thus providing a non-invasive method to measure cell division rate¹¹.

In this study, we used TPM to image the changes in chondrocyte autofluorescence in porcine nasal septal cartilage following ND:YAG laser ($\lambda=1.32 \mu\text{m}$) mediated stress relaxation. Moreover, we placed the cartilage in tissue culture for 4 days, and compared the TPM images of these specimens with images of native cartilage specimens maintained in culture for the same time duration. The objective of this study was to assess the metabolic activity and viability of chondrocytes



2. MATERIALS AND METHODS

2.1 Tissue harvest

Nasal septal cartilage was obtained from freshly euthanized pigs from a local abattoir (Lizaraga's Processing, Chino, CA) as previously described¹. The specimens were cut into rectangular slabs (25 x 10 x 2 mm) using a custom guillotine microtome¹, and stored in physiological saline at ambient temperature for about 2 hours prior to laser irradiation.

2.2 Biophysical measurements

Diffuse reflectance $I(t)$ from a HeNe probe laser ($\lambda = 632.8$ nm, 15mW, Melles Griot, Irvine, CA), radiometric surface temperature $S_s(t)$, internal stress $\sigma(t)$ were measured during laser irradiation as previously described (Figure 3)¹. The specimens were irradiated with a Nd:YAG laser ($\lambda = 1.32$ μm , 50 Hz Pulse Repetition Rate, NewStar Lasers, Auburn, CA), delivered via a 600 μm core diameter multimode optical fiber. The laser spot size was estimated to be 5.4 mm (power density, 25 W/cm²). $S_s(t)$ was monitored using a thermopile sensor (Thermalert MI-40, response time of 120 ms (95%), spectral sensitivity of 7.6-18 μm , Raytek, Santa Cruz, CA). The detection system was calibrated as previously described³.

2.3 Experimental protocol

A schematic of the experimental protocol is illustrated in Figure 4. Cartilage specimens were divided into two experimental protocols: **group A**) imaged immediately following tissue harvest or laser irradiation, and **group B**) irradiated and then placed in tissue culture for 4 days prior to imaging. Specimens within each study group were irradiated one, two, or three times with the laser (with a cooling time interval of 5 minutes between each pulse). The duration of each laser exposure was determined by observation of the peak value for $I(t)$ on the read-out of the lock-in amplifier; the laser irradiation was

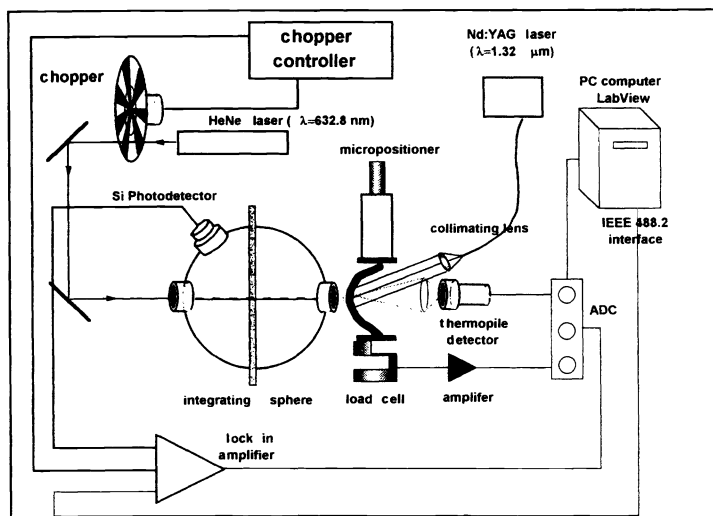


Figure 3: Schematic of experimental apparatus

terminated after the peak was identified. Thus, the time varied somewhat from sample to sample; however, the average irradiation time for the first, second, and third exposures were 5, 6, and 8 seconds, respectively.

Following irradiation, a 6 mm disc was excised from the irradiated region of the specimen, using a biopsy punch. Nicking an edge of the irradiated surface of the disc with a razor blade resulted in a discernible mark that in turn allowed specimen orientation.

2.4 Tissue culture

The excised discs were placed individually into 24 well culture plates and washed 3 times (15 minutes per wash) with an antibiotic rinse containing gentamicin (200 mg/L) and amphotericin B (22.4 mg/L) in phosphate buffered saline (PBS) (w/o calcium and magnesium). The samples were then

incubated (37°C, 5% CO₂) in Dulbecco's Modified Eagle's Medium (DMEM) (Life Technologies/Gibco, Grand Island, NY) containing 10% fetal calf serum (FCS), gentamicin (10 mg/mL), penicillin (100 μg/mL), streptomycin (100 μg/mL), and L-glutamine (29.2 g/mL). After 4 days in culture, the specimens were imaged using TPM.

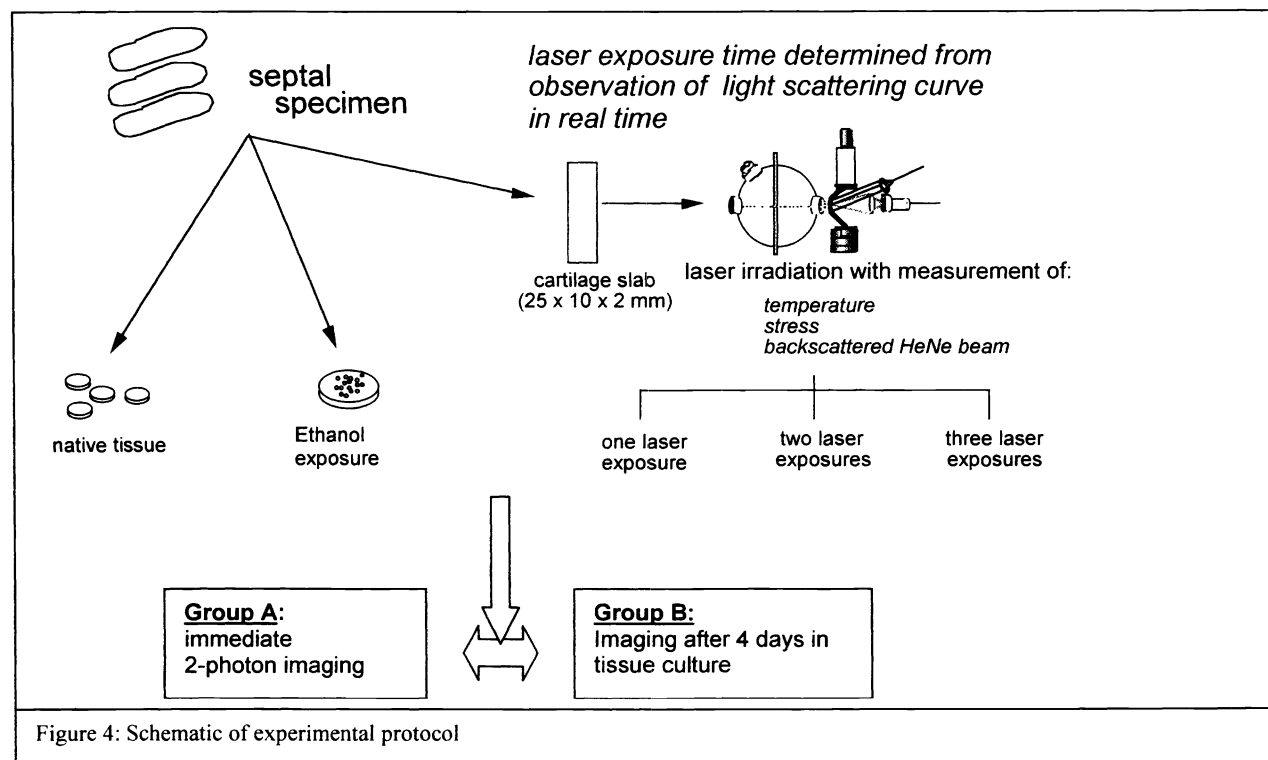


Figure 4: Schematic of experimental protocol

2.5 TPM imaging

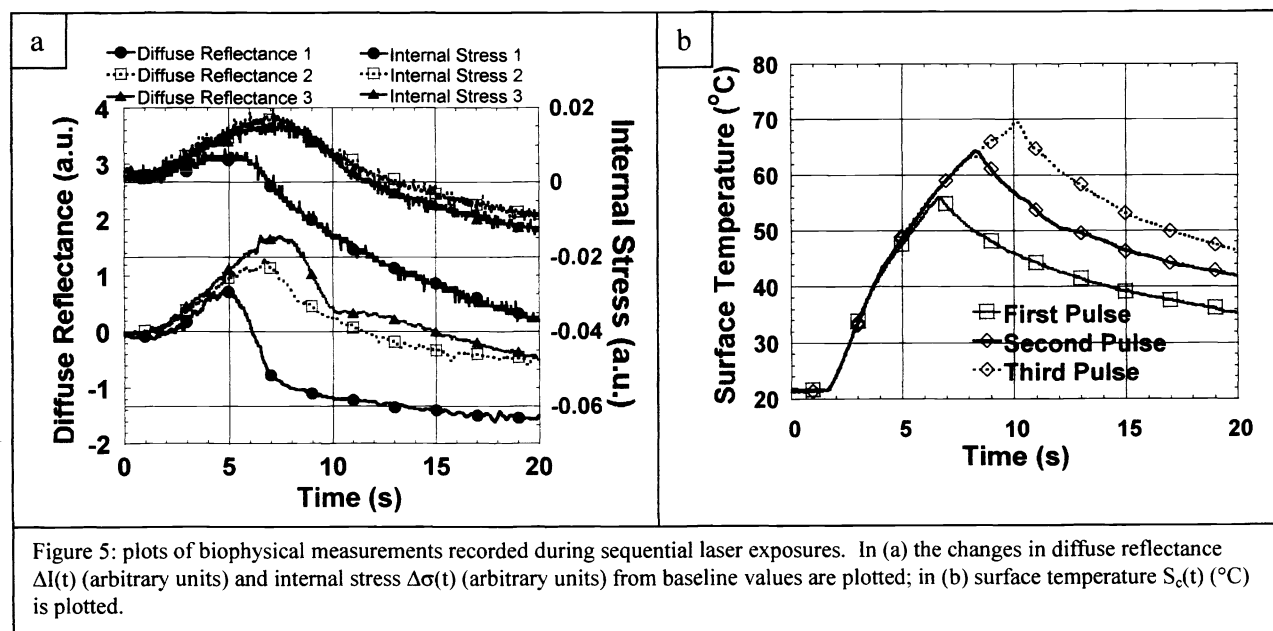
The TPM device in our laboratory is based on the system constructed by So et al at the Laboratory for Fluorescence Dynamics (LFD) at the University of Illinois at Urbana, Champagne. The system contains a 5W Verdi laser (Coherent,

Santa Clara, CA), which acts as a pump for the two photon, pulsed excitation source, Titanium: Sapphire (Ti: Al₂O₃) laser (Mira 900F, Coherent, Santa Clara, CA). Neutral density filters are used to control the average power after the Ti: Sapphire laser, so that the low powers necessary for cell survival could be maintained at the sample, while still maintaining sufficient peak power for two-photon excitation to occur. A mode-locked, 100 femtosecond, 76 MHz pulse train exiting the Ti: Sapphire laser is expanded and collimated using two lenses to overfill the back aperture of the microscope objective. **TPM** was performed using a mode-locked 780nm beam to optimally detect fluorescence from endogenous metabolic components such as **NADH**, **NADPH**, and flavoproteins in the 400-500 nm spectral region. The sample was placed on an inverted Zeiss Axiovert 100 microscope (Zeiss, Thornwood, NY). A small drop of PBS is used to cover the sample, and to minimize refractive mismatches. The Ti: Sapphire beam is scanned across the sample, using a PC-controlled X-Y scanner (Series 603X, Cambridge Technology, Inc., Watertown, MA). A Zeiss 63X, 1.2 N.A. water immersion objective (working distance of 200mm) was used.

The induced fluorescence from the tissue passes through a short pass dichroic beam splitter and is directed to a single photon counting detection system that consists of two PMTs (Hamamatsu Corp., Bridgewater, NJ) which are arranged perpendicularly, and separated by a long-pass dichroic beamsplitter. One PMT is optimized for green light (R7400P), and the other for red light (R7400P-01). This makes it possible to simultaneously detect fluorescence in two different wavelength regions.

TPM images of the specimens were obtained at depths of up to 150 microns (35 μm x 35 μm , lateral resolution). Images were obtained in cartilage specimens irradiated with one, two, or three sequential **ND:YAG** laser exposures, both immediately (within 180 minutes) following irradiation, and after 4 days in tissue culture. Native cartilage (negative control specimens) was imaged identically. Cartilage immersed in 50% EtOH for 20 minutes (and rehydrated in phosphate buffered saline for 10 min.) served as a positive control.

3. RESULTS



An example of the biophysical measurements recorded during photothermal heating is illustrated in **Figure 5**. The changes in diffuse reflectance $\Delta I(t)$ (a.u.) and internal stress $\Delta \sigma(t)$ (a.u.) from baseline values during sequential laser exposures are illustrated in **Figure 5 a**. For clarity, $S_c(t)$ is plotted independently (**Figure 5 b**). Peak surface temperatures of 56, 64, and 70°C were recorded during the first, second, and third laser pulses corresponding exposure times of 5.0, 6.6, and 8.3 sec. The time intervals between the onset of laser irradiation and the identification of a peak in $\Delta I(t)$ and $\Delta \sigma(t)$ increased with each successive irradiation as previously observed¹⁶. Because laser irradiation was terminated when the peak in $I(t)$ was

observed on the lock-in amplifier signal monitor, laser pulse durations were longer than the elapsed time at which the peaks in $\Delta I(t)$ and $\Delta \sigma(t)$ were observed. For the first two laser exposures, the maxima for both light and stress curves occurred simultaneously. In contrast, the peak for $\Delta I(t)$ precedes the peak for $\sigma(t)$ by about 0.4 seconds during the third laser exposure.

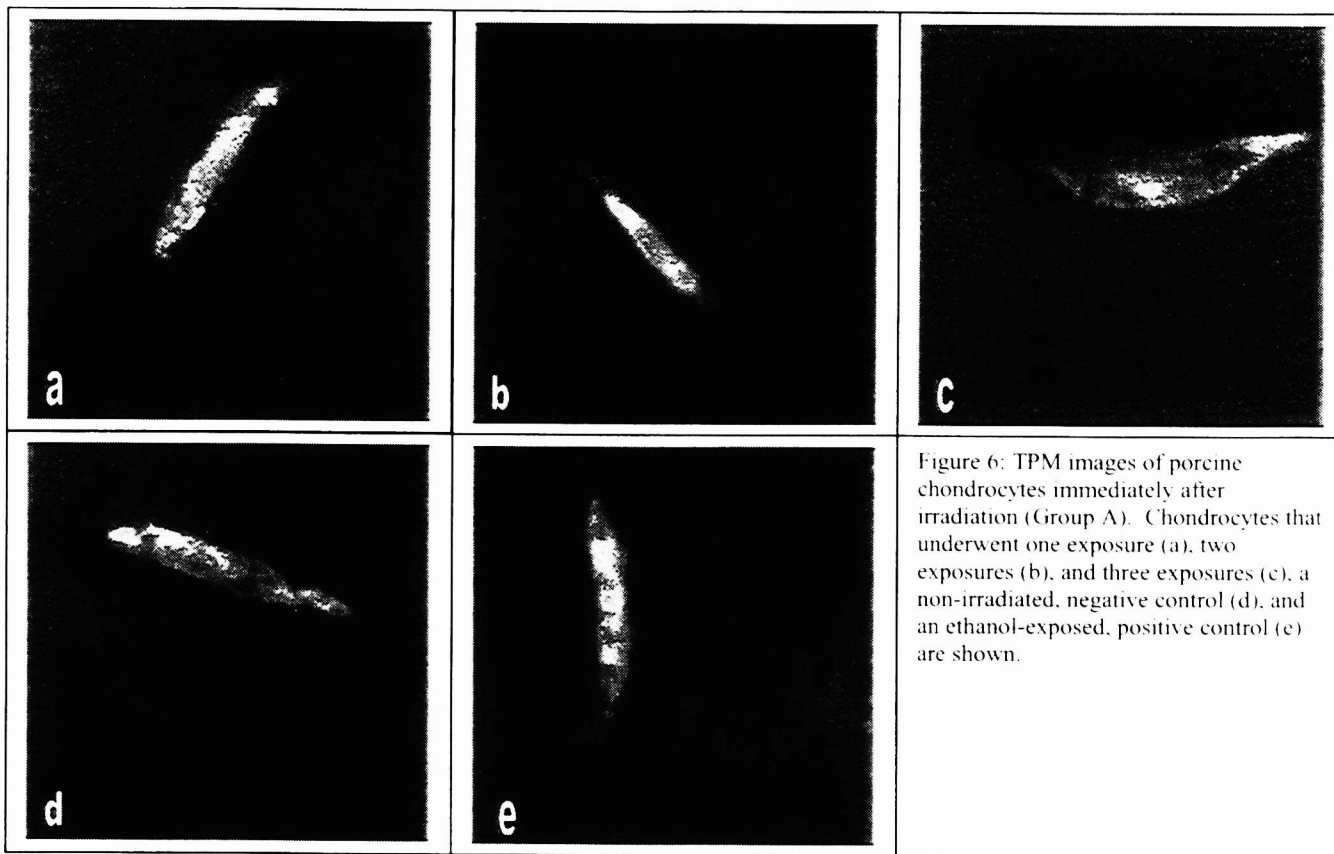


Figure 6: TPM images of porcine chondrocytes immediately after irradiation (Group A). Chondrocytes that underwent one exposure (a), two exposures (b), and three exposures (c), a non-irradiated, negative control (d), and an ethanol-exposed, positive control (e) are shown.

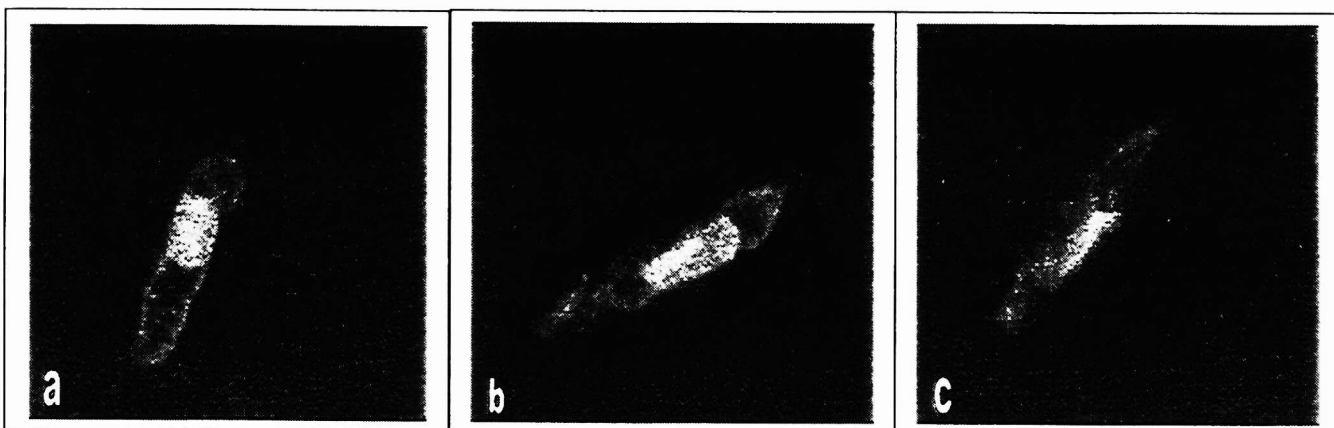


Figure 7: TPM images of chondrocytes following laser irradiation, and 4 days in tissue culture (Group B). Images of cells following 1 exposure (a), 3 exposures (b), and of a non-irradiated, negative control (c), are depicted.

Representative TPM images of chondrocytes within laser irradiated cartilage grafts are illustrated in Figures 6-7. $I(t)$, $S_c(t)$, and $\sigma(t)$ were recorded during the irradiation of each specimen with results similar to those illustrated in Figure 5. In Figure 6, TPM images of chondrocytes immediately after laser irradiation (group A) are illustrated. The montage is a composite of chondrocytes in cartilage specimens after (a) one, (b) two, or (c) three laser exposures, (d) non-irradiated native

tissue (negative control) and, (e) ethanol-denatured (positive control). Note the striking difference in fluorescence between native tissue and ethanol-denatured specimens. **Figure 7** consists of images of laser irradiated chondrocytes after being maintained in tissue culture for four days (**group B**): (a) one laser exposure, (b) three laser exposures; and (c) native tissue. Images of cartilage following two laser exposures were not obtained due to extensive specimen warping of these samples in culture that precluded TPM imaging.

Large oval regions with low signal intensity are identified in many cells (**Figure 6 c-d**, **Figure 7 a-c**), and are likely the nuclei, though it is possible that they may also be large lipid droplets, which are common in large chondrocytes¹⁵. Autofluorescence was observed diffusely in the cytoplasm in all specimens with the exception of the presumed nuclear regions; this high signal intensity (e.g. **Figure 6 b**) is likely due to the presence of mitochondria, which are rich with **NADH** and **NADPH**. Areas of relatively weak signal (e.g. **Figure 7 a**, where the nucleus in the lower half of the cell is surrounded by a thin, low intensity rim) may be regions where organelles such as the endoplasmic reticuli and Golgi apparatus are concentrated.

The lipid-rich cell membrane of the chondrocyte does not autofluoresce and hence forms a low signal intensity rim around the chondrocyte. The matrix immediately adjacent to the cell membrane often does not fluoresce as intensely as matrix further from the cell, and may delineate the *territorial matrix*. (see **Figures 6 a, b, d, e; 7 b**). The territorial matrix is known to have a high concentration of proteoglycans, and the concentration of collagen in this region may be lower, resulting in less fluorescence than other more collagen-rich regions of the matrix.

4. DISCUSSION

TPM was used to study the near-term changes in chondrocyte structure following laser irradiation, in order to determine whether significant structural/metabolic injury occurs within the cell after reshaping. Though studies examining tissue viability following laser irradiation have been performed, most of these only compare the physiologic or structural tissue response (as determined using histologic, biochemical, or molecular assays) with laser fluence and pulse duration^{17,18,19}. Our study differs from these investigations in that we monitored the thermal, optical, and mechanical properties of cartilage during laser irradiation, and thus were able to correlate the **TPM** images with changes in these biophysical properties. The onset of accelerated stress relaxation (representing a change in matrix structure) was used to terminate laser irradiation in each case.

In this pilot study, chondrocytes were imaged with **TPM** following **Nd:YAG** laser irradiation using parameters that result in tissue reshaping (stress relaxation). Functional images were constructed from the excitation of endogenous fluorophores providing a means to study chondrocyte metabolism. Prior studies have demonstrated that cellular emissions result primarily from the excitation of cellular **NADPH** and **NADH** (concentrated within the mitochondria), which provide an indirect measure of cellular respiration and metabolism²⁰. Flavoproteins located in the cytoplasm also function as fluorophores. Within the tissue matrix, collagen fibers readily fluoresce.

Few differences are observed between the laser-irradiated specimens (**Figure 6 a-c**) and native tissues (**Figure 6 d**) immediately after heating. Further, one, two, or three laser exposures does not alter the pattern of autofluorescence. In cells maintained in tissue culture (four days), there appears to be little difference in fluorescence between laser-irradiated specimens (**Figure 7 a, b**) and native specimens (**Figure 7 c**), or between the specimen exposed to (a) one laser pulse, or (b) three pulses. Chondrocytes imaged immediately and after four days also looked similar to one another.

Marked differences in fluorescence intensity between the positive (**Figure 6 e**) and negative controls (**Figure 6 d**) were observed. The ethanol-exposed chondrocytes diffusely fluoresce, when compared to native (**Figures 6 d; 7 c**) and irradiated cells (**Figures 6 a-c; 7 a-b**). This likely is indicative of ethanol-induced chondrocyte necrosis, which may involve processes such as enzymatic degradation, protein denaturation and degradation, and organelle lysis.

In contrast to previous work that measured chondrocyte proteoglycan (PTG) synthesis following laser irradiation¹⁶ (using a similar experimental protocol as this study), no "dose response" relationship between chondrocyte structure (**TPM** images) and laser dosimetry was observed. The lack of any clear difference between one, two, or three laser pulses is surprising, as previous studies have demonstrated that the metabolic rate of stromal keratocytes in humans increased markedly after the tissue was injured²¹. This may be in part due to the selective nature of microscopy in that only a limited

number of cells are observed; we focused primarily on imaging cells with intact cellular architecture. Functional/biochemical assay techniques (such as pulse-chase radiolabelling) measure the bulk response of a tissue to exogenous agents or changes in the physical environment (in this case, photothermal heating). Selective visualization of cells within the laser irradiated matrix may in part account for these observations. However, it is important to note that at least some cells in laser irradiated specimens did not look different from their respective controls.

5. CONCLUSION

Tissue viability can be evaluated using methods that characterize structural and functional aspects of cellular function. TPM is a unique method that allows for in vitro imaging to depths of several hundred microns where structural detail is provided based on concentration of fluorophores, principally molecules involved in respiratory transport. This preliminary investigation examined the changes in tissue autofluorescence following photothermal heating. In the sample of chondrocytes examined in this study, no differences in the pattern or intensity of fluorescence was observed between controls and irradiated specimens regardless of the number of laser exposures, and following four days in tissue culture. While these results are at variance with functional assays that demonstrate a dose response relationship, it is important to note that at least some chondrocytes are still intact with normal fluorescence patterns, despite repeated photothermal heating. Future work includes a thorough survey of irradiated tissue with TPM and the acquisition of fluorescence spectral information. This will allow identification of physiological changes within cells by looking at spectral alterations of endogenous fluorophores.

ACKNOWLEDGMENTS

The authors would like to acknowledge the technical assistance of Tatiana Krasieva, PhD, and Linda Li, M.D., as well as the comments and suggestions, of Chung-Ho Sun, PhD. This work was supported in part by the National Institutes of Health (1 K08 DC 00170-01, AR-43419, RR-01192, and HL-59472), Office of Naval Research (N00014-94-0874), The Whitaker Foundation (WF- 21025), and the Department of Energy (95-3800459).

REFERENCES

1. B.J.F. Wong, T.E. Milner, H.K. Kim, J.S. Nelson, E.N. Sobol, "Stress relaxation of porcine septal cartilage during ND:YAG laser irradiation," *Journal of Biomedical Optics* **3** (No. 4), 409-414, 1998.
2. B.J.F. Wong, T.E. Milner, A. Harrington, J. Ro, X. Dao, E.N. Sobol, J.S. Nelson, "Feedback controlled laser mediated cartilage reshaping," *Archives of Facial Plastic Surgery* **1** (No. 4), 1999.
3. B.J.F. Wong, T.E. Milner, B. Anvari, "Measurement of radiometric surface temperature and integrated back-scattered light intensity during feedback-controlled laser-assisted cartilage reshaping," *Lasers in Medical Science* **13**, 66-72, 1998.
4. V. Bagratashvili, E.N. Sobol, A. Sviridov, V.K. Popov, A. Omel'chenko, S.M. Howdle, "Thermal and diffusion processes in laser-induced stress relaxation and reshaping of cartilage," *J. Biomechanics* **30**, 813-817, 1997.
5. B.J.F. Wong, T.E. Milner, H.K. Kim, et al., "Critical temperature transitions in laser-mediated cartilage reshaping," *Proceedings SPIE* **3245**, 161-172, 1998.
6. E.N. Sobol, *Phase transformations and ablation in laser-treated solids*, John Wiley, New York, 316-322, 1995.
7. E.N. Sobol, A. Sviridov, V.V. Bagratashvili, et al., "Stress relaxation and cartilage shaping under laser radiation," *Proceedings SPIE* **2681**, 358-363, 1996.
8. E.N. Sobol, M. Kitai, N.S. Jones, A. Sviridov, T.E. Milner, B.J.F. Wong, "Theoretical modeling of heating and structure alterations in cartilage under laser radiation with regard of water evaporation and diffusion dominance," *Proceedings SPIE* **3254**, 54-63, 1998.
9. S.M. Potter, "Vital imaging: two photons are better than one," *Current Biology* **6** (No. 12), 1595-1598, 1996.
10. W. Denk, K. Svoboda, "Photon upmanship: why multiphoton imaging is more than a gimmick," *Neuron* **18**, 351-357, 1997.
11. D.W. Piston, B.R. Masters, W.W. Webb, "Three-dimensionally resolved NAD(P)H cellular metabolic redox imaging of the in situ cornea with two-photon excitation laser scanning microscopy," *Journal of Microscopy* **178** (Pt. 1), 20-27, 1995.
12. W. Denk, J.R. hold, G.M. Shepherd, D.P. Corey, "Calcium imaging of single stereocilia in hair cells: localization of transduction channels at both ends of tip links," *Neuron* **15**, 1311-1321, 1995.

13. B.D. Bennett, T.L. Jetton, G. Ying, M.A. Magnuson, D.W. Piston, "Quantitative subcellular imaging of glucose metabolism within intact pancreatic islets," *The Journal of Biological Chemistry* **271** (No. 7), 3647-3651, 1996.
14. D. Kleinfeld, P.P. Mitra, F. Helmchen, W. Denk, "Fluctuations and stimulus-induced changes in blood flow observed in individual capillaries in layers 2 through 4 of rat neocortex," *Proceedings of the National Academy of Sciences of the United States of America* **95**, 15741-6, 1998.
15. H.G. Burkitt, B. Young, J.W. Heath, P.J. Deakin, *Wheater's Functional Histology (3rd Ed.)*, ch. 10, Churchill Livingstone, New York, 1993.
16. B.J.F. Wong, T.E. Milner, H.K. Kim, K. Chao, C. Sun, E.N. Sobol, J.S. Nelson, "Proteoglycan synthesis in porcine nasal cartilage grafts following ND:YAG," *Photochemistry and Photobiology* **in press**, 2000.
17. Z. Wang, M.M. Pankratov, D.F. Perrault, S.M. Shapshay, "Endoscopic laser-assisted reshaping of collapsed tracheal cartilage: a laboratory study," *Annals of Otolaryngology, Rhinology, and Laryngology* **105**, 176-181, 1996.
18. Z. Wang, M.M. Pankratov, D.F. Perrault, S.M. Shapshay, "Laser-assisted cartilage reshaping: in vitro and in vivo animal studies," *Proceedings SPIE* **2395**, 296-302, 1995.
19. A. Sviridov, E.N. Sobol, V.V. Bagratashvili, et al., "In vivo study and histological examination of laser reshaping of cartilage," *Proceedings SPIE* **3590**, 222-228, 1999.
20. B. Chance, B. Thorell, "Localization and kinetics of reduced pyridine nucleotide in living cells by microfluorometry," *J. Biol. Chem.* **234**, 3044-3050, 1959.
21. M.B. McDonald, H.E. Kaufman, J.M. Frantz, S. Shofner, B. Salmeron, S.D. Klyce, "Excimer laser ablation in a human eye," *Arch Ophthalm.* **107**, 641-642, 1989.